Eur. Phys. J. B **59**, 311–318 (2007)
DOI: 10.1140/epjb/e2007-00295-y

THE EUROPEAN PHYSICAL JOURNAL B

Effect of step permeability on step instabilities due to alternation of kinetic coefficients on a growing vicinal face

M. Sato[a]
Information Media Center of Kanazawa University, Kakuma-cho, Kanazawa 920-1192, Japan

Received 28 January 2007 / Received in final form 25 June 2007
Published online 1st November 2007 –

Abstract. We study the effect of step permeability on step instabilities on a growing vicinal face. When alternation of kinetic coefficients is taken into account, pairing of steps occurs on the vicinal face. Irrespective of the step permeability, the step pairs are stable for a wandering instability. The bunching of step pairs occurs if the steps are impermeable. The bunch size increases with time as t^{β} with $\beta = 1/2$, which does not depend on the form of the repulsive interaction potential between steps. The repulsion influences the relation between the step distance in a bunch and the bunch size. When the repulsive potential ζ with the step distance l is given by $\zeta \sim l^{-\nu}$, the average step distance $\bar{l}$ in a bunch decreases as $\bar{l} \sim N^{-\alpha}$ with $\alpha = 1/(\nu+1)$. The exponents, β and α are the same as those in the bunching induced by the Ehrlich-Schowebel effect in growth.

PACS. 81.10.Aj Theory and models of crystal growth – 05.70.Ln Nonequilibrium and irreversible thermodynamics – 47.20.Hw Morphological instability – 68.35.Ct Interface structure and roughness

1 Introduction

A Si(001) surface is reconstructed by the dimerization of surface atoms. On the vicinal face tilted in the $\langle 001 \rangle$ direction, terrace T_B with the dimers parallel to steps and terrace T_A with dimers perpendicular to the steps appear alternately [1]. Due to the formation of the dimer row, surface diffusion becomes anisotropic. Surface diffusion parallel to the dimer rows is faster than that perpendicular to the dimer rows [2,3].

When a specimen is heated by direct electric current, step bunching [4–6] and step wandering [6] occur on the Si(001) vicinal face. The cause of the instabilities is considered to be the drift of adatoms induced by the current [7–14].

If we take account of the alternation of the anisotropic surface diffusion, the step wandering occurs with step-up drift [12], and the bunching occurs irrespective of the drift direction [7–14]. The results agree with experiments [4–6].

On the Si(001) vicinal face, in addition to the diffusion coefficients, the type of step changes alternately [2]. Step S_A, which is at the lower side of T_A, is smoother than S_B, which is at the lower side of T_B. The difference in the smoothness causes differences in step properties, e.g., the step stiffness of S_A is larger than that of S_B [15–17] and kinetic coefficient of S_A is probably smaller than that of S_B.

On the vicinal face, step bunching occurs at 490 °C in growth [18,19]. Frisch and co-worker [20] theoretically studied the step bunching. They used a step flow model, in which the anisotropy of the surface diffusion and the kinetic coefficients are changed alternately, and showed that the alternation of the kinetic coefficients causes the step bunching on the growing vicinal face.

In the study [20], they assume that the steps are impermeable. Without solidification, surface diffusion between neighboring terraces does not occur. The surface diffusion fields on neighboring terraces are independent of each other.

In general, if the kinetic coefficients are finite, the permeability can be incorporated in a macroscopic step flow model. Step permeability affects the condition which causes the step bunching. For example, in the drift-induced step instabilities on a Si(111) model, the drift direction to cause the instabilities changes with the step permeability [21–23]. In the present case, the permeability may also change the step behavior.

In this paper, bearing the growing Si(001) vicinal face in mind, we study the effect of the step permeability on step instabilities induced by alternation of kinetic coefficients. We neglect the alternation of anisotropy of surface diffusion. To see the effect of the step permeability clearly, we consider only two extreme cases: the vicinal face with perfectly permeable steps and that with impermeable steps. We show how the motion of the steps is changed by the step permeability. In Section 2, we introduce a step flow model. We study instabilities of the impermeable steps in Section 3, and those of the perfectly permeable steps in Section 4. We summarize the results and give brief discussions in Section 5.

[a] e-mail: sato@cs.s.kanazawa-u.ac.jp

2 Model

In our step flow model, alternation of the kinetic coefficients is taken into account. We consider a vicinal face with step distance l, where the y-direction is the step-down direction and the x-direction is parallel to the steps. When we neglect evaporation of adatoms, the diffusion equation of the adatom density $c(\boldsymbol{r},t)$ is given by

$$\frac{\partial c(\boldsymbol{r},t)}{\partial t} = \nabla \cdot \boldsymbol{j}(\boldsymbol{r},t) + F, \tag{1}$$

where $\boldsymbol{j}(\boldsymbol{r},t)$ is the adatom current and F is impingement rate of atoms. The adatom current in the vicinal face is expressed as

$$\boldsymbol{j} = -D_{\mathrm{s}} \left(\frac{\partial c}{\partial y}\hat{\boldsymbol{e}}_x + \frac{\partial c}{\partial x}\hat{\boldsymbol{e}}_y \right), \tag{2}$$

where $\hat{\boldsymbol{e}}_y$ is the unit vector in the y-direction, $\hat{\boldsymbol{e}}_x$ is that in the x-direction and D_{s} is the diffusion coefficient. To focus on the effect of the kinetic coefficient, we neglect the alternation of anisotropy of surface diffusion.

Solidification of adatoms and melting of solid atoms occur at step positions. At the ith step, solidification occurs if the adatom density is higher than the equilibrium value, $c_{\mathrm{eq}}^{(i)}$, and melting occurs if the adatom density is lower than $c_{\mathrm{eq}}^{(i)}$. The boundary conditions at the step are given by [24]

$$K_i(c|_{y_i+} - c_{\mathrm{eq}}^{(i)}) = -\hat{\boldsymbol{n}} \cdot \boldsymbol{j}|_{y_i+} + P_i(c|_{y_i+} - c|_{y_i-}), \tag{3}$$

$$K_i(c|_{y_i-} - c_{\mathrm{eq}}^{(i)}) = \hat{\boldsymbol{n}} \cdot \boldsymbol{j}|_{y_i-} + P_i(c|_{y_i-} - c|_{y_i+}), \tag{4}$$

where $\hat{\boldsymbol{n}}$ is the unit vector normal to the step, K_i is the kinetic coefficient and P_i is the parameter for the step permeability. y_i represents the step position and the subscript $+(-)$ indicates the lower (upper) side of the step. The kinetic coefficient changes with the type of the step: $K_i = K_{\mathrm{A}}$ for $\mathrm{S_A}$ and $K_i = K_{\mathrm{B}}$ for $\mathrm{S_B}$. Since $\mathrm{S_B}$ is rougher than $\mathrm{S_A}$, we assume that K_{B} is larger than K_{A}. The parameter P_i should be changed with the type of steps, but to see the effect of the step permeability clearly, we also assume $P_{\mathrm{A}} = P_{\mathrm{B}} = P$.

In equations (3) and (4), the term on the left hand side represents the number of adatoms solidified at the steps. By the interaction potential ζ_i between steps, the equilibrium adatom density, $c_{\mathrm{eq}}^{(i)}$ is given by

$$c_{\mathrm{eq}}^{(i)} = c_{\mathrm{eq}}^{0} \left(1 + \frac{\Omega}{k_{\mathrm{B}}T}\frac{\partial \zeta_i}{\partial y_i} \right), \tag{5}$$

where c_{eq}^{0} is the equilibrium adatom density of an isolated step and Ω is the atomic area. On the Si(001) vicinal face, ζ_i is given by [25]

$$\zeta_i = -A(\ln l_i + \ln l_{i-1}), \tag{6}$$

where the terrace width l_i is given by $l_i = y_{i+1} - y_i$.

In equations (3) and (4), the first term on the right hand side represents the adatom current to the steps, and the second term represents the number of adatoms passing through the step without solidification. When $P \to \infty$, the step is called perfectly permeable. Without solidification, adatoms move to neighboring terraces. The difference in the adatom density vanishes. When $P \to 0$, the step is called impermeable. The diffusion fields on neighboring terraces are separated at the step position and independent of each other. The adatoms move to the neighboring terraces after solidification at the step. If the kinetic coefficient is finite, a gap in the adatom density appears.

By solving the diffusion equation, equation (1) with the boundary conditions, equations (3) and (4), the adatom density is determined and the velocity V_i of the step is obtained as

$$V_i = \Omega \hat{\boldsymbol{n}} \cdot (\boldsymbol{j}|_{y_i-} - \boldsymbol{j}|_{y_i+}). \tag{7}$$

In general, the permeability P_i depends on the type of step, and is also related to the step kinetics. Since the kink density at $\mathrm{S_B}$ is more than that at $\mathrm{S_A}$ [15–17], solidification at $\mathrm{S_A}$ is easier than at $\mathrm{S_B}$. The permeability of $\mathrm{S_A}$ may be larger than that of $\mathrm{S_B}$. However, if the difference in the step permeability is taken into account, the situation becomes more complicated. Our aim is to see the effect of the permeability clearly. Thus, we assume the permeability of $\mathrm{S_A}$ is equal to that of $\mathrm{S_B}$, and we treat two extreme cases: the instabilities with perfectly permeable steps and those with impermeable steps.

3 Instabilities with impermeable steps

We first study step instabilities of impermeable steps. To study the stability for the step bunching, we assume that the steps are straight. When we use the one-dimensional model, the velocity V_i of the ith step is given by

$$V_i = \frac{\Omega K_i[Fl_{i-1}\{K_{i-1}l_{i-1} + 2D_{\mathrm{s}}\} + 2D_{\mathrm{s}}K_{i-1}\Delta c_{i-1}]}{2\{D_{\mathrm{s}}(K_i + K_{i-1}) + K_iK_{i-1}l_{i-1}\}} + \frac{\Omega K_i[Fl_i\{K_{i+1}l_i + 2D_{\mathrm{s}}\} - 2D_{\mathrm{s}}K_{i+1}\Delta c_i]}{2\{D_{\mathrm{s}}(K_i + K_{i+1}) + K_iK_{i+1}l_i\}}, \tag{8}$$

where the difference Δc_i of the equilibrium adatom density is given by $\Delta c_i = c_{\mathrm{eq}}^{(i+1)} - c_{\mathrm{eq}}^{(i)}$.

On a vicinal face with $l_i = l$, the effect of the repulsion on the equilibrium adatom density cancels from equation (5): $c_{\mathrm{eq}}^{(i)} = c_{\mathrm{eq}}^{(i+1)} = c_{\mathrm{eq}}^{0}$ and Δc_i vanishes. The step velocities, V_{A}^{0} of $\mathrm{S_A}$ and V_{B}^{0} of $\mathrm{S_B}$ are given by

$$V_{\mathrm{A}}^{0} = \frac{K_{\mathrm{A}}Fl(K_{\mathrm{B}}l + 2D_{\mathrm{s}})}{D_{\mathrm{s}}(K_{\mathrm{A}} + K_{\mathrm{B}}) + K_{\mathrm{A}}K_{\mathrm{B}}l}, \tag{9}$$

$$V_{\mathrm{B}}^{0} = \frac{K_{\mathrm{B}}Fl(K_{\mathrm{A}}l + 2D_{\mathrm{s}})}{D_{\mathrm{s}}(K_{\mathrm{A}} + K_{\mathrm{B}}) + K_{\mathrm{A}}K_{\mathrm{B}}l}. \tag{10}$$

Since we have assumed that K_{B} is larger than K_{A}, $\mathrm{S_B}$ advances faster than $\mathrm{S_A}$. An equidistant array of step pairs separated by $\mathrm{T_B}$ is produced. By the difference in the terrace width, the equilibrium adatom density c_{B} of $\mathrm{S_B}$ is

larger than c_A of S_A. From equations (5) and (6), the difference $\Delta c(= c_B - c_A)$ in the equilibrium adatom density is expressed as

$$\Delta c = \frac{2\Omega c_{eq}^0 A}{k_B T}\left(\frac{1}{l-\Delta l} - \frac{1}{l+\Delta l}\right) \approx \frac{4\Omega c_{eq}^0 A}{k_B T l^2}\Delta l, \quad (11)$$

where $\Delta l = (l_A - l_B)$ represents the difference in the terrace width.

Since the steps move as step pairs, S_A and S_B advance with the same velocity. From the condition $V_A = V_B$, Δc is expressed as

$$\frac{2K_A K_B \Delta c}{(K_B - K_A)F} = \frac{D_s(K_A + K_B)l}{D_s(K_A + K_B) + K_A K_B l} + \frac{K_A K_B l_A l_B}{D_s(K_A + K_B) + K_A K_B l}, \quad (12)$$

where l_B is the width of T_B and l_A is that of T_A. From equations (8) and (12), the velocity V_{pair} of the step pair is given by $V_{pair} = \Omega F l$. The difference between V_{pair} and $V_A^0(V_B^0)$ are expressed as

$$V_B^0 - V_{pair} = -(V_A^0 - V_{pair}) = \frac{FlD_s(K_A - K_B)}{D_s(K_A + K_B) + K_A K_B l}. \quad (13)$$

By the formation of step pairs, the velocity of S_A becomes faster and that of S_B becomes slower. V_{pair} is the average of V_A^0 and V_B^0.

With a set of parameters, the step distance in a pair is uniquely determined. When the repulsion is strong, the step pair is loosely bound. Δl is much smaller than the average step distance l. From equation (11), Δl is expressed as

$$\Delta l = \frac{k_B T l^2 (K_B - K_A)F}{8K_A K_B \Omega A c_{eq}^0}. \quad (14)$$

When the repulsion is weak, the step pair is tightly bound and Δl is comparable to l. If l_A is so narrow that $l_A \ll (K_A + K_B)D_s/2K_A K_B l$, from equation (12) Δc is approximated as

$$\Delta c = \frac{(K_B^2 - K_A^2)FD_s l}{2D_s K_A K_B\{D_s(K_A + K_B) + K_A K_B l\}}. \quad (15)$$

On the other hand, when l_A is much narrower than l_B, Δc is expressed as

$$\Delta c = \frac{2\Omega c_{eq}^0 A}{k_B T}\left(\frac{1}{l_A} - \frac{1}{l_B}\right) \approx \frac{2\Omega c_{eq}^0 A}{k_B T l_A}, \quad (16)$$

in which we use equation (5). From equations (15) and (16), the step distance l_A is approximately given by

$$l_A \approx \frac{4K_A K_B\{D_s(K_A + K_B) + K_A K_B l\}\Omega A c_{eq}^0}{FD_s l(K_B^2 - K_A^2)k_B T}. \quad (17)$$

Hereafter, we study the instability of an equidistant train of tight step pairs. For small T_A, the adatom current is much smaller than that for large T_B. The stability of the equidistant array of step pairs is determined by the adatom current on large T_B. We give a small fluctuation to the width of T_B without changing l_A. We assume the narrow T_B with width $l_B - \delta l_B$ and wide T_B with $l_B + \delta l_B$ appear alternately. Since the repulsion is weak and l_B is large, the change of Δc is neglected. When the width of the upper side terrace is $l_B + \delta l_B$, the change of the velocity δV_{pair} of the step pair is given by

$$\delta V = \mu F \delta l_B, \quad (18)$$

where the coefficient μ is expressed as

$$\mu = \frac{D_s^2(K_B^2 - K_A^2)}{\{D_s(K_A + K_B) + 2K_A K_B\}} \times \frac{1}{\{D_s(K_A + K_B) + K_A K_B\}}. \quad (19)$$

When the difference in terrace width is small [20], δV is proportional to F^2. In the present case, the tight step pairs are formed and the difference in terrace width is large. δV is proportional to F in equation (18).

Since K_B is larger than K_A, the coefficient μ is positive in equation (19). If $\delta l_B < 0$, i.e., the upper side terrace is smaller than the lower side terrace, the step pair is decelerated. If $\delta l_B > 0$, the step pair is accelerated. Therefore, the equidistant array of step pairs is unstable against the fluctuation, and the pairing of step pairs occurs. When the similar process occurs successively, large bunches may be formed.

To study the behavior of an unstable array, we carry out numerical simulations. In our simulations, we use $\zeta_i = A_\nu(l_i^{-\nu} + l_{i-1}^{-\nu})$ or $\zeta_i = -A_0(\ln l_i + \ln l_{i-1})$ as the repulsive interaction potential. Figure 1 shows the time evolution of step positions with the logarithmic repulsive potential. The dimensionless time $\tilde{t}$, the dimensionless step position

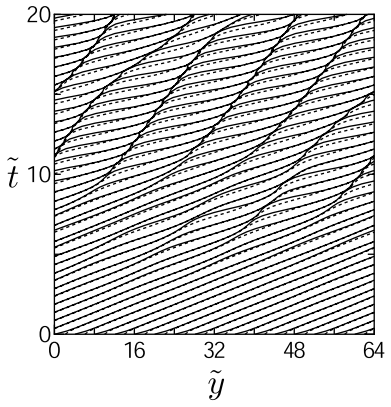

Fig. 1. Time evolution of step positions. The number of steps is 32 and the system width is 64 with periodic boundary conditions.

$\tilde{y}$ and the dimensionless impingement rate $\tilde{F}$ are defined as

$$\tilde{t} = \frac{tK_{\rm B}^{\nu+3}\Omega^2\tilde{A}_\nu c_{\rm eq}^0}{D_{\rm s}^{\nu+2}k_{\rm B}T}, \tag{20}$$

$$\tilde{y} = \frac{yK_{\rm B}}{D_{\rm s}}, \tag{21}$$

$$\tilde{F} = \frac{FD_{\rm s}^2k_{\rm B}T}{K_{\rm B}^3\Omega\tilde{A}_\nu c_{\rm eq}^0}, \tag{22}$$

where $\nu = 0$ and $\tilde{A}_\nu = A_0$ for the logarithmic repulsive potential and $\tilde{A}_\nu = \nu A_\nu$ for other potentials. The dimensionless impingement rate is $\tilde{F} = 20$ and the ratio of the kinetic coefficients is $K_{\rm A}/K_{\rm B} = 0.2$. The number of steps is 32 and the scaled system size is 64 with the periodic boundary condition. The dotted lines are the orbits of $S_{\rm A}$ and the solid lines are those of $S_{\rm B}$.

Initially, the steps are equidistant with small random fluctuation. In an early stage, $S_{\rm B}$ advances faster than $S_{\rm A}$, and pairing of the steps occurs. The step pairs are not broken into single steps. The equidistant array of the step pairs is unstable and step bunching occurs. In a later stage, collisions of step pairs to bunches occurs successively. When a step pair collides to a bunch from the upper side, another step pair separates from the lower side. By repeating the collision and separation, bunches gradually grow. In step bunching, the step pairs do not break and are stable, which agrees with a previous study [26].

The adatom density at the lower side of the step pair is higher than at the upper side. In the equidistant array of the pairs, the difference $\Delta c_{\rm pair}$ in the adatom density is given by

$$\Delta c_{\rm pair} = \frac{Fl_{\rm A}(K_{\rm B} - K_{\rm A})}{2\{2D_{\rm s}(K_{\rm A} + K_{\rm B}) + K_{\rm A}K_{\rm B}l_{\rm A}\}}, \tag{23}$$

where we assumed that step distance in a pair is small. On a vicinal face consisting of single steps with step distance $l_{\rm A}$, the same gap is given if the kinetic coefficients are $K_{\rm A}/2$ in the upper side of the step and $K_{\rm B}/2$ in the lower side of the step. Since the steps move as step pairs, we can regard a step pair as an effective single step with the negative Ehrlich-Schwoebel (ES) effect [27,28]. Then, growth law is expected to be the same as that for step bunching, induced by the ES effect on the growing vicinal face [29].

Figure 2 shows the time evolution of the size of the largest bunch, which is averaged over 10 runs. The system size is twice as large as that in Figure 1. Irrespective of the exponent ν of the repulsive interaction potential, the bunch grows as t^β with $\beta \approx 1/2$. The form of the repulsion affects the step distance in the bunch. Figure 3 shows the dependence of the average step distance $\bar{l}$ on the number $N_{\rm max}$ of steps in the largest bunch. With increasing the bunch size $N_{\rm max}$, the average step distance decreases as $\bar{l} \sim N_{\rm max}^{-\alpha}$ with $\alpha = 2/(\nu+1)$. The exponent α with the logarithm repulsion ($\nu = 0$) seems to be slightly smaller than $\alpha = 2$, but the exponents α and β agree with those in theoretical studies [26,29,30].

In the above analysis, we assume that the steps are straight. In the two-dimensional system, however, the other type of step instability, step wandering may occur during growth. Since the evaporation of adatoms is neglected in the present case, we use the same analysis as that in reference [31]. We consider the equidistant train of steps whose normal direction is tilted from y-axis with an angle θ. In growth, the vicinal face is unstable and the pairing of steps occurs. When the step pairs are formed, the total current $J_x^{\rm A}$ in the x-direction on $T_{\rm A}$ and $J_x^{\rm B}$ on $T_{\rm B}$ are given by

$$J_x^{\rm A} = -\mu_{\rm A}\tan\theta, \tag{24}$$

$$J_x^{\rm B} = -\mu_{\rm B}\tan\theta. \tag{25}$$

The coefficients $\mu_{\rm A}$ and $\mu_{\rm B}$ are expressed as

$$\mu_{\rm A} = -\frac{D_{\rm s}\tilde{l}_{\rm A}[F\tilde{l}_{\rm A}(K_{\rm B} - K_{\rm A}) + 2K_{\rm A}K_{\rm B}\Delta\tilde{c}]}{2[(K_{\rm A} + K_{\rm B}) + K_{\rm A}K_{\rm B}\tilde{l}_{\rm A}]}, \tag{26}$$

$$\mu_{\rm B} = -\frac{D_{\rm s}\tilde{l}_{\rm B}[F\tilde{l}_{\rm A}(K_{\rm A} - K_{\rm B}) - 2K_{\rm A}K_{\rm B}\Delta\tilde{c}]}{2[(K_{\rm A} + K_{\rm B}) + K_{\rm A}K_{\rm B}\tilde{l}_{\rm B}]}, \tag{27}$$

where $\tilde{l}_{\rm A} + \tilde{l}_{\rm B} = l\cos\theta$ and $\Delta\tilde{c}$ is the difference of the adatom density on the tilted system.

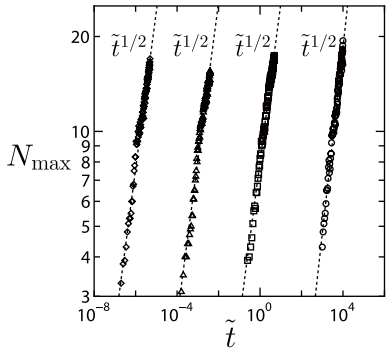

Fig. 2. Time evolution of the size of the largest bunch, which is averaged over 10 runs: ◯ with $\nu = 0$ and $\tilde{F} = 2 \times 10$, □ with $\nu = 2$ and $\tilde{F} = 2 \times 10^{-2}$, △ with $\nu = 4$ and $\tilde{F} = 2 \times 10^{-5}$ and ♢ with $\nu = 6$ and $\tilde{F} = 2 \times 10^{-8}$. The number of steps is 64 and the system width is 128.

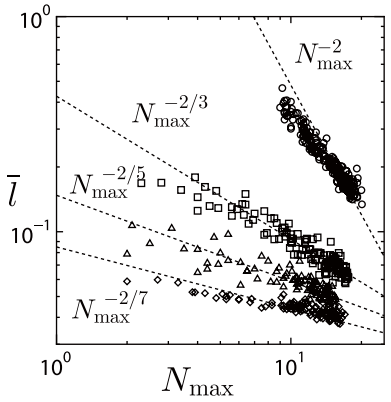

Fig. 3. Dependence of average step distance in the largest bunch on the number $N_{\rm max}$ of the step, which is averaged over 10 runs. The parameters and symbols are the same as those in Figure 2.

When the difference of the terrace width is small, the total current $J_x = J_x^{\rm A} + J_x^{\rm B}$ per step pair is given by

$$J_x = -\frac{F^2(K_{\rm B}-K_{\rm A})k_{\rm B}Tl^4}{16K_{\rm A}K_{\rm B}\Omega c_{\rm eq}^0 A} \times \frac{\tan\theta\cos^4\theta}{\{D_{\rm s}(K_{\rm A}+K_{\rm B})+K_{\rm A}K_{\rm B}l\cos\theta\}}. \quad (28)$$

When an in-phase wandering occurs and the fluctuation is expressed as $\zeta(x,t)$, the time evolution of the fluctuation is given by

$$\frac{\partial\zeta}{\partial t} = -\Omega\frac{\partial J_x}{\partial x} \approx \gamma\frac{\partial^2\zeta}{\partial x^2}, \quad (29)$$

where we use $\partial\zeta/\partial x = \tan\theta$. In equation (29), the coefficient γ is expressed as

$$\gamma = \frac{F^2(K_{\rm B}-K_{\rm A})k_{\rm B}Tl^4}{16K_{\rm A}K_{\rm B}c_{\rm eq}^0 A[D_{\rm s}(K_{\rm A}+K_{\rm B})+K_{\rm A}K_{\rm B}l]^2}. \quad (30)$$

If $l_{\rm A}$ is so narrow that $J_x \approx J_x^B$, the coefficient γ is expressed as

$$\gamma = \frac{Fl^2(K_{\rm B}-K_{\rm A})[2(K_{\rm A}+K_{\rm B})+K_{\rm A}K_{\rm B}l]}{2[(K_{\rm A}+K_{\rm B})+K_{\rm A}K_{\rm B}l]^2}. \quad (31)$$

Irrespective of the width of $l_{\rm A}$, the coefficient γ is positive. Then, with the alternation of the kinetic coefficients, the step wandering does not occur on the growing vicinal face.

4 Step instabilities with perfectly permeable steps

When the steps are perfectly permeable, the parameter $P \to \infty$. The boundary conditions, equations (3) and (4) are expressed as

$$c|_{y_i+} = c|_{y_i-} = c_{\rm s}, \quad (32)$$

$$2K_i(c_{\rm s} - c_{\rm eq}^{(i)}) = \hat{\boldsymbol{e}}_y \cdot \left(\boldsymbol{j}|_{y_i-} - \boldsymbol{j}|_{y_i+}\right). \quad (33)$$

The step velocity is given by

$$V_i = 2\Omega K_i(c_{\rm s} - c_{\rm eq}^{(i)}). \quad (34)$$

On the vicinal face, the step velocities, $V_{\rm A}$ and $V_{\rm B}$ are the same as those with the impermeable steps, which are given by equations (9) and (10). Since $S_{\rm A}$ advances faster than $S_{\rm B}$, step pairs separated by $T_{\rm B}$ are formed. When the width of $T_{\rm B}$ is $l_{\rm B}$ and that of $T_{\rm A}$ is $l_{\rm A}$, the velocities are given by

$$V_{\rm A} = \frac{\Omega K_{\rm A}l(2D_{\rm s}Fl + K_{\rm B}l_{\rm A}l_{\rm B} + 2K_{\rm B}\Delta c)}{(K_{\rm A}+K_{\rm B})D_{\rm s}l + K_{\rm A}K_{\rm B}l_{\rm A}l_{\rm B}}, \quad (35)$$

$$V_{\rm B} = \frac{\Omega K_{\rm B}l(2D_{\rm s}Fl + K_{\rm A}l_{\rm A}l_{\rm B} - 2K_{\rm A}\Delta c)}{(K_{\rm A}+K_{\rm B})D_{\rm s}l + K_{\rm A}K_{\rm B}l_{\rm A}l_{\rm B}}. \quad (36)$$

From the condition $V_{\rm A} = V_{\rm B}$, the difference Δc in the equilibrium adatom density is obtained as

$$\Delta c = \frac{Fl(K_{\rm B}-K_{\rm A})}{2K_{\rm B}K_{\rm A}}, \quad (37)$$

which does not depend on Δl. The form of Δc is different from that in the impermeable case, which is given by equation (12). The velocity of the step pair, however, is the same as that in the impermeable case and given by $V_{\rm pair} = \Omega Fl$.

On surface consisting of equidistant step pairs, from equation (37), the total adatom currents $J_{\rm A}$ on $T_{\rm A}$ and $J_{\rm B}$ on $T_{\rm B}$ are given by

$$J_{\rm A} = \frac{l_{\rm B}D_{\rm s}[2K_{\rm A}K_{\rm B}\Delta c + F(K_{\rm A}-K_{\rm B})l]}{2[D_{\rm s}l(K_{\rm A}+K_{\rm B}) + K_{\rm A}K_{\rm B}l_{\rm A}l_{\rm B}]} = 0, \quad (38)$$

$$J_{\rm B} = \frac{l_{\rm A}D_{\rm s}[-2K_{\rm A}K_{\rm B}\Delta c + F(K_{\rm B}-K_{\rm A})l]}{2[D_{\rm s}l(K_{\rm A}+K_{\rm B}) + K_{\rm A}K_{\rm B}l_{\rm A}l_{\rm B}]} = 0. \quad (39)$$

Step bunching occurs when the average adatom current in the upper side direction increases with increasing the inclination of the surface [32]. In the present case, the average adatom currents are absent on both $T_{\rm A}$ and $T_{\rm B}$. Then, step bunching probably does not occur.

To examine the stability of the array of step pairs, we use a two-dimensional square lattice model and carry out a Monte Carlo simulation. The algorithm is similar to that in a previous study [33], in which the model is in the limit of large ES effect. Diffusion between neighboring terraces is forbidden. In our model, the ES effect is neglected and adatom diffusion between neighboring terrace without solidification is allowed.

Adatoms and solid atoms are distinguished in our model. We repeatedly choose a solid atom, which is at a step position, or an adatom. When an adatom is chosen, the adatom hops into a neighboring site with the probability 1/4 if the site is empty. In our algorithm, the diffusion constant $D_{\rm s} = 1$. In one diffusion trial, the increase Δt of time is expressed as $\Delta t = 1/4N_{\rm a}$, where $N_{\rm a}$ is the number of adatoms. After a few diffusion trials, impingement of adatoms is periodically carried out. In the continuum limit, the distribution of adatom density obeys equation (1) if the adatom density is low. In our model, solidification of adatoms and melting occurs only at step positions, and the nucleation of two dimensional islands and vacancies is forbidden. After the hopping trial, the solidification trial is successively carried out if the adatom attaches to a step from the lower side. When a solid atom is selected, a melting trial is carried out. The melted atom stays in the same site as an adatom. For $S_{\rm B}$ steps, the probability p_+ of solidification and p_- of melting are given by

$$p_\pm = \left[1 + \exp\left(\frac{\Delta E_{\rm s} \mp \phi}{k_{\rm B}T}\right)\right]^{-1}. \quad (40)$$

$\Delta E_{\rm s} = \epsilon\times$ (the increment of the step perimeter), where ϵ is half of the bonding energy. ϕ is the decrease in the chemical potential by solidification. For $S_{\rm A}$ steps, the probabilities are given by $p_k p_\pm$, where the parameter p_k represents

the ratio of the kinetic coefficients and $p_k < 1$. With equilibrium adatom density $c^0_{\rm eq}$, the frequency of solidification is equal to that of melting at a kink site. Irrespective of the type of step, the equilibrium adatom density is given by

$$c^0_{\rm eq} = \left[1 + \exp\left(\frac{\phi}{k_{\rm B}T}\right)\right]^{-1}. \tag{41}$$

The estimation of kinetic coefficients from microscopic models has been carried out in previous papers [34–36]. Solidification and melting mainly occur at kink sites. When the step kink density is high, we can roughly estimate the kinetic coefficient.

The number $\Delta N_{\rm s}$ of solidified adatoms and the number $\Delta N_{\rm m}$ of melting atoms are roughly estimated as

$$\Delta N_{\rm s} = \frac{c_{\rm s} p_{\rm s} L}{N_{\rm a}}, \tag{42}$$

$$\Delta N_{\rm m} = \frac{(1-c_{\rm s}) p_{\rm m} L}{N_{\rm a}}, \tag{43}$$

where $c_{\rm s}$ is the adatom density at the step, L is the system length, $p_{\rm s}$ is the average solidification probability, and $p_{\rm m}$ is the average melting probability. The probabilities are approximately the same as those at a kink site. For S_B steps, the net number of solidification atoms per unit length is given by

$$\begin{aligned}\frac{\Delta N_{\rm s} - \Delta N_{\rm m}}{L} &= \frac{c_{\rm s} p_{\rm s} + (1-c_{\rm s}) p_{\rm m}}{N_{\rm a}} \\ &= \frac{c_{\rm s}(p_{\rm s} + p_{\rm m}) - p_{\rm m}}{N_{\rm a}} \\ &= \frac{c_{\rm s} - c^0_{\rm eq}}{N_{\rm a}} = 4\Delta t (c_{\rm s} - c^0_{\rm eq}),\end{aligned} \tag{44}$$

where we used $p_{\rm m} = c^0_{\rm eq}$ at the kinks and $\Delta t = 1/4N_{\rm a}$. By comparison of equations (3) and (4) with equation (44), the kinetic coefficient of S_B is estimated as $K_{\rm B} = 4$. For S_A, the kinetic coefficient is given by $K_{\rm A} = 4p_k$.

In our model, we introduced the probability p_k to change the kinetic coefficient of S_A, but we can change the kinetic coefficient by changing the step energy ϵ of S_A. When the step energy of S_A is larger than that of S_B, the step stiffness of S_A is larger than that of S_B. Thus, the kink density of S_A is smaller than that of S_B, and K_A becomes smaller than K_B. However, if we change the step energy, we cannot use the rough estimation given by equation (44). Thus, we introduced the probability p_k and changed the kinetic coefficient. In our model, the step stiffness $\tilde{\beta}$ of S_A is the same as that of S_B, and given by

$$\tilde{\beta} = \frac{2k_{\rm B}T}{a} \sinh^2 \frac{\epsilon}{2}, \tag{45}$$

where a is the lattice constant. In simulation, we set $a = 1$.

If solidification does not occur, the adatom stays at the same position. The adatom coming from the upper terrace stays on the lower terrace. By the next diffusion trial, the adatom can move to the neighboring terrace.

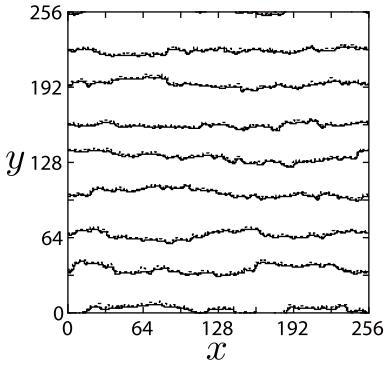

Fig. 4. Snapshot of the step pairs. The system size is 256×256 with periodic boundary condition and the number of steps is 32.

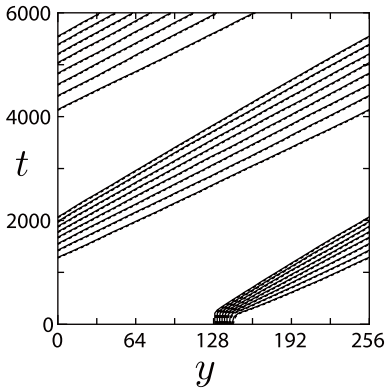

Fig. 5. Time evolution of positions of steps. Parameters are the same as those in Figure 4

If a difference in the adatom density between the upper terrace and the lower terrace is present, the gap can be removed by the diffusion. Since the extra potential barrier is absent in the diffusion between the neighboring terraces, irrespective of the type of step, $c|_- = c|_+ = c_{\rm s}$ in the continuum limit. Thus, the steps are perfectly permeable in our model. If we change the steps to impermeable steps, the adatom motion at the step positions is more complicated as in reference [22]

Figure 4 shows a snapshot of the surface. The dotted lines are S_A and the solid lines are S_B. Parameters are $\epsilon/k_{\rm B}T = 2.0$, $\phi/k_{\rm B}T = 1.5$, $F = 0.005$ and $p_k = 0.1$. The step stiffness $\tilde{\beta}$ is $\tilde{\beta}/k_{\rm B}T = 2.7$. Since the kink density is $\sim (\tilde{\beta}/k_{\rm B}T)^{-1} = 0.37$, the steps have many kinks and the estimation by equation (44) is valid.

Initially, the steps are straight and equidistant. When impingement starts, the pairing of steps occurs. The equidistant array of steps seems to be stable, and step bunching does not occur. To examine the stability of an equidistant array of step pairs, we started the simulation with an isolated large bunch. Figure 5 shows the time evolution of the average step positions. In the initial stage, the step pair at the front side of the step bunch successively separates from the bunch, and the bunch is broken to step pairs. Thus, on the vicinal face with permeable steps, the

equidistant array of step pairs is stable and step bunching does not occur.

In Figure 4, step wandering does not seem to occur. When the step is perfectly permeable, the adatom currents are $J_A = J_B = 0$. If the system is tilted, the total adatom current J_x in the x-direction is absent, and $\partial\zeta/\partial x = 0$. From the same analysis as that in Section 3, we can show that the step pairs are marginal compared to in-phase step fluctuation. When the Gibbs-Thomson effect is taken into account, the fluctuation is suppressed and the array of step pairs is stable for step wandering.

5 Summary and discussions

In this paper, taking a growing Si(001) vicinal face as an example, we studied the effect of step permeability on step instabilities induced by the alternation of kinetic coefficients. Irrespective of the step permeability, the growing vicinal face is unstable and pairing of steps occurs. The pairs are stable for a wandering instability. The stability for step bunching changes with step permeability. The equidistant array of step pairs is stable if the step is perfectly permeable, but the step bunching occurs if step is impermeable. In experiment [18,19], step bunching occurs at 490 °C. Then, the steps are probably impermeable on the growing Si(001) vicinal face.

In our simulation, the number N of steps in the largest bunch increases as $N \sim \tilde{t}^{\beta}$ with $\beta = 1/2$, and the average step distance $\bar{l}$ in the bunch decreases as $\bar{l} \sim N^{-\alpha}$ with $\alpha = 2/(\nu+1)$. The exponents, β and α are the same as those in step bunching by the negative ES effect on the growing vicinal face [29,30]. In our model, since the steps move as step pairs, the step pair is regarded as single step with the negative ES effect [27,28,26]. Then, the exponents, α and β agree with those in previous studies [29,30].

In a previous study [20], step pairing does not occur when the impingement rate is larger than the critical value. In our model, from equation (17), the step distance in a pair l_A decreases as $l_A \sim F^{-1}$, and the critical impingement rate does not appear. In the previous paper [20], they set $l_A = 1$ and found the suitable l_B. Then, with large impingement rate, l_A cannot be smaller and the formation of tight step pairs is forbidden, which explains the disagreement.

With the alternation of the kinetic coefficients, step wandering does not occur irrespective of the step permeability. In our model, the alternation of the diffusion coefficients, which causes the step wandering with the drift of adatoms [12], is neglected. The alternation may cause step wandering on the growing vicinal face. We are currently studying the possibility of step wandering caused by alternation of the diffusion coefficients.

In a real system, when the adatoms attach to steps, they migrate along the step and solidify at the kink sites. When the kink density is high, the majority of adatoms can solidify, and the step is impermeable. When the kink density is low, many adatoms cannot find the kink sites. The adatoms detach from the step without solidification, and the step is permeable. The step permeability is changed by the kink density. Since the kinetic coefficient is related to the kink density, the permeability depends on the kinetic coefficients. Though we assumed that the permeability of S_A is the same as that of S_B in our model, we should change the permeability of S_A from that of S_B. However, to derive the relation between the kinetic coefficient and the permeability, the detailed parameters of the materials are necessary and the situation becomes complicated. Then, for the first step, we changed the permeability independently of the kinetic coefficients.

By using this simple model, we studied only the two extreme cases: the instabilities with perfectly permeable steps and those with impermeable steps. When the steps are impermeable and the kinetic coefficient is finite, large bunches are formed and the growth laws in impermeable steps are consistent with experiment [26]. Thus, the steps on Si(001) vicinal faces at low temperature may be regarded as impermeable steps. However, we studied only the two extreme causes. To carry out more quantitative comparison with experiments [18,19,26], we have to study more general causes.

This work was supported by Grant-in-Aid for Scientific Research from the Japan Society for the Promotion of Science.

References

1. D.J. Chadi, Phys. Rev. Lett. **59**, 1691 (1987)
2. Y.-W. Mo, M.G. Lagally, Surf. Sci. **248**, 313 (1991)
3. Y.-W. Mo, J. Kleiner, M.B. Webb, M.G. Lagally, Surf. Sci. **268**, 275 (1992)
4. L.V. Litvin, A.B. Krasilnikov, A.V. Latyshev, Surf. Sci. **244**, L121 (1991)
5. A.L. Latyshsv, L.V. Litvin, A.L. Aseev, Appl. Surf. Sci. **130-132**, 139 (1998)
6. J.-F. Nielsen, M.S. Pettersen, J.P. Pelz, Surf. Sci. **480**, 84 (2001)
7. S. Stoyanov, Jpn. J. Appl. Phys. **29**, L659 (1990)
8. A. Natori, H. Fujimura, H. Yasunaga, Jpn. J. Appl. Phys. **92**, 1164 (1992)
9. A. Natori, H. Fujimura, M. Fukuda, Appl. Surf. Sci. **60/61**, 85 (1992)
10. M. Sato, M. Uwaha, Y. Saito, J. Cryst. Growth **237-239**, 43 (2002)
11. M. Sato, M. Uwaha, T. Mori, Y. Hirose, J. Phys. Soc. Jpn **72**, 2850 (2003)
12. M. Sato, M. Uwaha, Y. Saito, Y. Hirose, Phys. Rev. B **67**, 125408 (2003)
13. M. Sato, T. Mori, M. Uwaha, Y. Hirose, J. Phys. Soc. Jpn **73**, 1827 (2004)
14. M. Sato, M. Uwaha, Y. Hirose, J. Phys. Soc. Jpn **75**, 043601 (2006)
15. N.C. Bartelt, R.M. Tromp, E.D. Williams, Phys. Rev. Lett. **73**, 1656 (1994)
16. N. Akutsu, Y. Akutsu, Surf. Sci. **92**, 92 (1997)
17. N. Akutsu, Y. Akutsu, Phys. Rev. B **57**, R4233 (1998)
18. C. Schelling, G. Springholtz, F. Schäffler, Phys. Rev. Lett. **83**, 995 (1999)

19. J. Mysliveček, C. Schelling, F. Schäffler, G. Springholz, P. Šmilauer, J. Krug, B. Voigtländer, Surf. Sci. **520**, 193 (2002)
20. T. Frisch, A. Verga, Phys. Rev. Lett. **94**, 226102 (2005)
21. J.J. Métois, S. Stoyanov, Surf. Sci. **440**, 407 (1999)
22. M. Sato, M. Uwaha, Y. Saito, Phys. Rev. B **62**, 8452 (2000)
23. O. Pierre-Louis, Surf. Sci. **529**, 114 (2003)
24. M. Ozdemir, A. Zangwill, Phys. Rev. B **45**, 3718 (1992)
25. O.L. Alerhand, D. Vanderbilt, R.D. Meade, J.D. Joannopoulos, Phys. Rev. Lett. **61**, 1973 (1988)
26. A. Pascale, I. Berbezier, A. Ronda, A. Videcoq, A. Pimpinelli, Appl. Phys. Lett. **89**, 104108 (2006)
27. R.L. Schwoebel, E.J. Shipsey, J. Appl. Phys. **37**, 3682 (1966)
28. G. Ehrlich, G. Hudda, J. Chem. Phys. **44**, 1039 (1966)
29. M. Sato, M. Uwaha, Surf. Sci. **493**, 494 (2001)
30. A. Pimpinelli, V. Tonchev, A. Videcoq, M. Vladimirowa, Phys. Rev. Lett. **88**, 206103 (2002)
31. F. Gillet, O. Pierre-Louis, C. Misbah, Eur. Phys. J. B **18**, 519 (2000)
32. M.D. Johnson, C. Orme, A.W. Hunt, D. Graff, J. Sudijono, L.M. Sander, B.G. Orr, Phys. Rev. Lett. **72**, 116 (1993)
33. Y. Saito, M. Uwaha, Phys. Rev. B **49**, 10677 (1994)
34. O. Pierre-Louis, Phys. Rev. Lett. **87**, 106104 (2001)
35. S.N. Filimonov, Yu. Yu. Hervieu, Surf. Sci. **553**, 133 (2004)
36. L. Balykov, Axel Voigt, Phys. Rev. E **72**, 022601 (2005)